



23 and volume models and provides accurate information; therefore, it is appropriate for  
24 determining potential rainfall impact over long time periods. Specifically, we applied  
25 this methodology to the daily rainfall time series from the San Fernando Observatory  
26 (1870-2010) in southwest Europe. An interannual aggressiveness risk series was  
27 generated, which allowed analysis of its evolution and determination of the temporal  
28 variability. The results imply that environmental management can use data from long-  
29 term historical series as a reference for decision making.

30 **KEY WORDS:** Aggressiveness; Rainfall erosivity; Land use; Environmental risk;  
31 Southwest Europe

32

## 33 1. Introduction

34 One of the features of the rainfall regime in a Mediterranean climate is the inter- and  
35 intra-annual irregularity (García-Barrón *et al.*, 2013). Inter-decadal climate studies help  
36 to explain the causes of terrain alteration over time (Diodato *et al.*, 2008). Rainfall  
37 erosivity causes a loss of fertile soil, damage to agriculture and infrastructure and water  
38 pollution and is influenced by changes in rainfall patterns (Martín-Fernández &  
39 Martínez-Nuñez, 2011; Sánchez-Moreno *et al.*, 2014) and by predictable effects of  
40 climate change (Diodato *et al.*, 2011). In this study, we consider aggressiveness risk as a  
41 potential estimate of the physical effects of rainfall on soil dynamics *sensu* Fournier  
42 (1960). Our view is that aggressiveness risk is an appropriate environmental indicator  
43 and directly related to erosion and associated with the incidence of torrents, floods,  
44 landslides, displacement, etc. (Gregori *et al.*, 2006). Therefore, knowledge of this  
45 variable over long periods is particularly useful for the management of water resources,  
46 soil conservation, agricultural planning and the development of environmental policy.  
47 Moreover, annual estimates of aggressiveness risk enable the comparison of orders of  
48 magnitude among different observation sites at different times. This environmental  
49 indicator is based on daily rainfall records and does not include other aspects related to  
50 erosion such as slope length, soil types, wind activity, land use, etc.

51 For the direct calculation of soil erosion, the universal soil loss equation (USLE)  
52 has been frequently used (Wischmeier & Smith, 1978). Specifically, the rainfall  
53 erosivity, or *R* factor, depends on the energy of every rainfall episode (Panagos *et al.*,  
54 2015). The *R* factor is an accepted instrument for local erosion measurement,  
55 successively updated and empirically endorsed by means of field measurements (Renard  
56 *et al.*, 1997). Models such as the USLE and RUSLE were originally developed for

57 detailed scale application in the farming sector, so their application on a regional scale  
58 presents some limitations (Terranova *et al.*, 2009). Although USLE is one of the most  
59 widely used erosivity models worldwide, it has some limitations because the  
60 estimations of soil erosion do not fit the empirical measures of sedimentation, and the  $R$   
61 erosivity factor does not explicitly incorporate direct runoff of water, which affects the  
62 accuracy of the model (Kinnell, 2010). Additionally, the spatial distribution tends to  
63 overestimate the  $R$  factor at regional or river basin levels (Hernando & Romana, 2016),  
64 and its is not recommended in areas different from those in which it was developed  
65 without an analysis of the validity of the equations.

66 In the specific case of the study of rainfall aggressiveness effects, two  
67 complementary approaches are taken: intensity models are based on sub-hourly rainfall  
68 records, and volume models are based on monthly rainfall records. This model refers to  
69 the different partial accumulations of rainfall. That is, it does not take into account the  
70 number, the duration and the rainfall amount of each episode, so that it's based  
71 exclusively on the total monthly rainfall. Nevertheless for the direct calculation of the  
72 rainfall erosivity in large areas, it is desirable to make use of high frequency rainfall  
73 records collected by nearby weather stations during a period longer than twenty years  
74 (Angulo-Martinez *et al.*, 2009). However, except for modern automatic weather  
75 stations, traditional observatories have no high-frequency series with sub-hourly  
76 records. On the other hand, volume models are based on monthly rainfall records that  
77 are extensively available in most countries. In this case, the regular use of the  
78 aggressiveness index in environmental studies (Fournier, 1960), subsequently modified  
79 by Arnoldus (1980) as the Modified Fournier Index ( $I_{FM}$ ) and complemented with the  
80 Precipitation Concentration Index ( $I_{PC}$ ) developed by Oliver (1980), is remarkable.

81 Both estimations for calculating the intensity of rainfall aggressiveness present  
82 limitations. The drawback of the intensity models is the lack of adequate time series  
83 records, and that of the volume models is the imprecision in the treatment of heavy rain  
84 episodes because they are based on finer timescale resolutions. The amount of  
85 precipitation is not the only relevant parameter; its temporal distribution is also relevant,  
86 as studies on Mediterranean river basins in the NE Iberian Peninsula (Sánchez-Canales  
87 *et al.*, 2015) and in the SW Iberian Peninsula (Sousa *et al.*, 2009) have made evident.  
88 Various studies have compared the results obtained using intensity models (the  $R$  factor  
89 of USLE) to those obtained using volume models. In the Iberian Peninsula, the Institute  
90 for the Conservation of Nature (ICONA, 1988) under the Spanish Ministry of  
91 Agriculture proposed an empirical relationship that locally associates the  $R$  factor with  
92 the  $I_{FM}$  index. Additionally, a high correlation between the  $R$  factor and the monthly  
93 and/or annual precipitation parameters, including the Fournier Index, has been obtained  
94 in various geographic areas, such as in the Mediterranean area (Diodato & Bellocchi,  
95 2007; Taguas *et al.*, 2013), East Asia (Lee & Heo, 2011; Yue *et al.*, 2014) and the  
96 tropical zone (Sanchez-Moreno *et al.*, 2014). In the USA, Renard & Freid (1994)  
97 proposed regression equations that calculate the  $R$  factor from  $I_{FM}$ . Additionally,  
98 Loureiro & Couthino (2001) estimated the  $R$  factor based on the monthly rainfall  
99 aggressiveness in southern Portugal, and Da Silva (2004) estimated the same in Brazil.

100 In this study, we propose to estimate the aggressiveness risk by means of a  
101 single annual parameter that improves the limitations of models based only on monthly  
102 records (volume models) and those based on sub-hourly records (intensity models). We  
103 used a method based on the daily scaled reformulation of the traditional indices of  
104 aggressiveness,  $I_{FM}$  and  $I_{PC}$ , that provides more accurate results. The method also allows

105 numerous investigations because there are many weather stations that have large time  
106 series of daily data. This Estimated Annual Aggressiveness Risk ( $R_A$ ) is calibrated  
107 locally by means of regression equations with respect to the erosivity  $R$  factor for a  
108 period of simultaneity. Backwards extrapolation of the resulting function generates the  
109 corresponding time series of the aggressiveness risk. Recently, García-Barrón *et al.*  
110 (2015) have synthesized in this parameter the aggressiveness risk using  $I_{FM}$  and  $I_{PC}$  to  
111 study trends in river basins of the Iberian Peninsula. In this article, we propose two main  
112 objectives:

- 113 a) To define and calculate a single annual parameter based on daily records  
114 that synthetically estimates the rainfall aggressiveness risk.
- 115 b) To apply this methodology to a study area with a Mediterranean climate  
116 to analyse the temporal behaviour and deduce patterns in the evolution of  
117 the rainfall aggressiveness risk.

## 118 **2. Study area and data**

119 We chose the South-Atlantic region of the Iberian Peninsula for the methodological  
120 application, which is based on a long period and can help to draw conclusions about the  
121 potential risks of rainfall on the land. Spain is one of the countries most severely  
122 affected by soil erosion in the European Mediterranean region due to extreme spatial  
123 and temporal variations in its physical environment, with frequent periods of drought  
124 and torrential rainfall (Solé, 2006). The importance of erosion in the Mediterranean is  
125 related to the long history of human activity in a region characterized by low annual  
126 precipitation, the occurrence of intense rainstorms and long-lasting droughts, high  
127 evapotranspiration, the presence of steep slopes and the occurrence of recent tectonic

128 activity, together with the recurrent use of fire, overgrazing and farming (García-Ruiz et  
129 al., 2013).

130 The southwestern Iberian Peninsula falls within the domain of the Mediterranean  
131 climate, although it is influenced by an oceanic effect because of its proximity to the  
132 Atlantic Ocean. The average annual rainfall is approximately 600 mm (average values  
133 are substantially higher in the mountain range separating the watersheds of the  
134 Guadiana and Guadalquivir rivers). Rainfall is subject to marked inter-annual  
135 irregularity, with great oscillations in annual totals that include multi-year periods of  
136 drought (Aguilar, 2007). In general, the profile of the intra-annual precipitation shows  
137 an asymmetric unimodal curve, ascending in autumn and descending smoothly from  
138 winter to summer, when it reaches its minimum.

139 The Royal Observatory of the Spanish Navy (ROA) located in San Fernando  
140 (province of Cadiz, at the southern tip of the Iberian Peninsula) includes the oldest  
141 active weather station in Spain; rainfall records have been recorded since 1805 and  
142 accessible daily data since 1870. Because of these long-term and high-quality records,  
143 different studies have used ROA data as a reference to characterize the rainfall regime  
144 (Rodrigo, 2002; Martin-Vide & Lopez-Bustins, 2006) and the inter- and intra-annual  
145 behaviour (García-Barrón *et al.*, 2013) of rainfall in the study area.

146 The meteorological stations located in the province or district capitals of Spain  
147 and Portugal have been selected to quantify the level of regional representation of the  
148 ROA rainfall series (Figure 1). Data from the Spanish stations were provided by the  
149 Spanish Meteorological Agency (AEMET), and data from the Portuguese stations were  
150 provided by the Portuguese Sea and Atmosphere Institute (IPMA). The weather stations  
151 are distributed over different geographical areas as follows: Cadiz, Huelva and Faro in

152 the coastal zone, Cordova and Seville in the Guadalquivir valley, and Badajoz and Beja  
 153 in the Guadiana basin (Figure 1).



154

155 **Figure 1.** Map showing the locations of the meteorological stations used in the study  
 156 area.

157 These series are homogeneous and have no missing data (Almarza *et al.*, 1996;  
 158 García-Barrón *et al.*, 2013). We have chosen the period 1961-1990, recommended by  
 159 the World Meteorological Organization, for comparing the ROA rainfall records to  
 160 those of every selected regional station. Table 1 shows the representativeness of the  
 161 ROA compared to every selected observatory in the area. To determine the  
 162 representativeness, we calculated the proportionality of the average annual rainfall  
 163 between the ROA and every selected station, the R-Pearson coefficient of the annual  
 164 totals of the respective rainfall series and the R-Pearson coefficient of the monthly  
 165 average of the intra-annual distribution.

166 **Table 1.** Proportionality coefficient and annual and interannual correlation between the  
 167 San Fernando Observatory (ROA) and the selected regional stations.



Observatories	Country	Institution	Latitude and Longitude	Annual average rate	R-Pearson Interannual	R-Pearson Intra-annual
San Fernando (ROA)	Spain	ROA	36° 27' 56" N 6° 12' 20" W	-	-	-
Cadiz	Spain	AEMET	36° 32' 01" N 6° 17' 58" W	1.04	0.96	1.00
Huelva	Spain	AEMET	37° 16' 30" N 6° 54' 35" W	1.03	0.94	0.98
Faro	Portugal	IPMA	37° 01' 00" N 7° 55' 59" W	1.04	0.76	0.97
Seville	Spain	AEMET	37° 25' 05" N 5° 42' 30" W	1.02	0.85	0.98
Cordova	Spain	AEMET	37° 50' 40" N 4° 51' 02" W	0.96	0.86	0.98
Badajoz	Spain	AEMET	38° 43' 02" N 6° 49' 45" W	1.02	0.72	0.94
Beja	Portugal	IPMA	38° 00' 56" N 7° 51' 55" W	0.92	0.70	0.94

168

169 Table 1 shows that although the total rainfall differs among neighbouring  
170 stations and in those within the same basin, the intra- and inter-annual behaviour is  
171 similar. The high correlation of the results obtained in Table 1 shows that the region  
172 studied has the same climate and is subject to the same synoptic conditions. This  
173 corroborates the conclusions of previous studies on rainfall in the southwestern Iberian  
174 Peninsula (García-Barrón *et al.*, 2011). Therefore, we assume that the general rainfall  
175 regime of the ROA sufficiently characterizes the Atlantic southern zone of the Iberian  
176 Peninsula for analysis of its temporal variability. Consequently, this study estimated the  
177 behaviour of the temporal evolution of the aggressiveness risk using daily rainfall  
178 records of the ROA from 1870 to 2010. Absolute homogeneity tests were applied to the  
179 annual series with AnClim software (Stepanek, 2007) and the Standard Normal

180 Homogeneity Test (SNHT) for a single series (Alexandersson, 1986). The results  
 181 support the quality of the series. The rainfall-measuring unit was mm.

182 The calculation of the regional erosivity, the  $R$  factor of USLE, was provided by  
 183 the Environmental Information Network of the Ministry of Environment of the  
 184 Andalusia Government. The automatic weather station at Cadiz (Table 1) was selected  
 185 for calculating the  $R$  factor (Rodríguez Surián & Sánchez Pérez, 1995) because of the  
 186 quality of its rainfall records. Because of their proximity (<12 km) and similar  
 187 geographical conditions, the rainfall records of the stations at Cadiz and San Fernando  
 188 (ROA) are similar and consistent. This allowed us to use the results of the  $R$  factor as an  
 189 element of correspondence to establish the relationship with the  $R_A$  in the study area  
 190 during the simultaneity period (1991-2010).

### 191 3. Methodology

192 The methodology proposed is based jointly on  $I_{FM}$  and  $I_{PC}$ . As a new contribution, the  
 193 classic definition of these indices was altered to perform calculations using daily  
 194 precipitation data. Both indices were used to define a unique annual parameter, the  
 195 Estimated Annual Aggressiveness Risk ( $R_A$ ), that calculates, accurately and  
 196 synthetically, the potential effect of rainfall aggressiveness for every year in the study  
 197 area using one single variable. This makes it possible to generate a multi-annual series  
 198 to establish its time evolution in the study area.

199 From the daily rainfall series obtained for each  $N$  years of records,  $R_A$  is  
 200 obtained using the indices ( $I_{FM}^*$ ,  $I_{PC}^*$ ) as follows:

$$201 \quad R_A = \varphi (I_{FM}^*, I_{PC}^*) \quad (1)$$

202 where  $I_{FM}^*$  is a daily scale of the Modified Fournier Index,

$$203 \quad I_{FM}^* = (\sum p_d^2)/P \quad (2)$$

204 and  $I_{PC^*}$  is a daily scale of the Precipitation Concentration Index,

$$205 \quad I_{PC^*} = 100 (\sum p_d^2) / P^2 \quad (3)$$

206 where  $p_d$  is the daily precipitation ( $d = 1, 2, \dots, 365$ ) and  $P$  is the corresponding  
 207 total annual precipitation.  $I_{FM^*}$  units are the same as those of rainfall, and  $I_{PC^*}$  is  
 208 dimensionless.

209 To mathematically estimate the values of  $R_A$ , we established the connection with  
 210 the erosivity data  $R$  of USLE for a period of simultaneous records. By linear regression,  
 211 we obtain

$$212 \quad \varphi (I_{FM^*}, I_{PC^*}) = R + \xi \quad (4)$$

213 where the function  $\varphi$  is determined, with  $\xi$  being the residual deviation.

214 Using backwards extrapolation, the repeated application of the resulting  
 215 equation to the corresponding annual values of  $I_{FM^*}$  and  $I_{PC^*}$  produces the  $R_A$  interannual  
 216 series for the period. The procedure has a feature that the estimation of the  $R_A$  risk is  
 217 measured in the same units and with the same scale as the  $R$  factor of USLE.

218 The use of daily data to calculate  $R_A$  incorporates the environmental impact  
 219 caused by heavy daily rains. It also allows the use of long time series from many  
 220 weather stations. Therefore, the proposed method to calculate the annual  $R_A$  improves  
 221 the quality of the evaluation compared to the traditional volume models and  
 222 incorporates calibration with respect to the intensity models. In view of this, we believe  
 223 that the proposal is innovative, as it combines the advantages of both models and  
 224 overcomes some of their limitations.

225  $I_{FM^*}$  has a high dependence on total annual rainfall. In general,  $I_{PC^*}$  also depends  
 226 on total annual rainfall. However, if every daily record of one year is proportional  
 227 (multiple or submultiple) to those of another year, then  $I_{PC^*}$  is independent of the total

228 rainfall and only depends on the intra-annual distribution of rainfall. Therefore, if we  
 229 consider that daily rainfall ( $p_{di}$ ) of the year  $n$  has its corresponding proportion ( $p'_{di} = k$   
 230  $p_{di}$ ) in the year  $n'$  (although not necessarily in the same order), where  $k$  is a constant,  
 231 then the respective Fournier indices are proportional to each other, whereas the  
 232 concentration indices are equal:

$$233 \quad I'_{FM*} = k \cdot I_{FM*} ; \quad I'_{PC*} = I_{PC*} \quad (5)$$

234 The theoretical limits of  $I_{PC*}$  are as follows: a higher value of 100 based on the  
 235 assumption that all the annual rainfall occurs in one day and a minimum of 0.27 based  
 236 on the assumption of a uniform equipartition among the days of the year. Therefore,  
 237 high values of  $I_{PC*}$  indicate a heavy rainfall for a few days and thus a higher erosive  
 238 power, whereas low values of  $I_{PC*}$  indicate light rainfall distributed along many days  
 239 and thus less aggressiveness.

240 The analysis mechanism to reveal the temporal irregularity of the generated  $R_A$   
 241 series uses the linear trend and the variation and disparity coefficients of the entire  
 242 series. The inter-annual behaviour is analysed using the accumulated deviations of  $R_A$   
 243 with respect to the  $\mu_N$  average of the whole series, the variability for mobile periods and  
 244 the Specific Disparity Index.

245 The accumulated value, to the year, was obtained by the sum of the annual  
 246 deviations of  $R_A$  with respect to the  $\mu_N$  average of the whole series, extended to all the  
 247 preceding  $i$  years:

$$248 \quad A_n = (\sum \delta_i) / \mu_N \quad (6)$$

249 where  $\delta_i = (R_{Ai} - \mu_N)$ , for  $i = 1, 2, \dots, n; n \leq N$

250 The  $R_A$  variation coefficient of the N-year complete series (1870-2010) is  
 251 defined as the quotient of the standard deviation and the corresponding average  $\mu_N$ :

252 
$$V_N = \sigma_N / \mu_N \quad (7)$$

253 Similarly, the moving variation coefficient for periods of eleven years  
 254 corresponding to the year  $n$  ( $1 \leq n \leq N$ ) is defined as the quotient of the standard  
 255 deviation of the partial subseries formed by the reference year  $n$  and the previous ten  
 256 years and their corresponding average:

257 
$$V_{(11)n} = \sigma_{(n, n-10)} / \mu_{(n, n-10)} \quad (8)$$

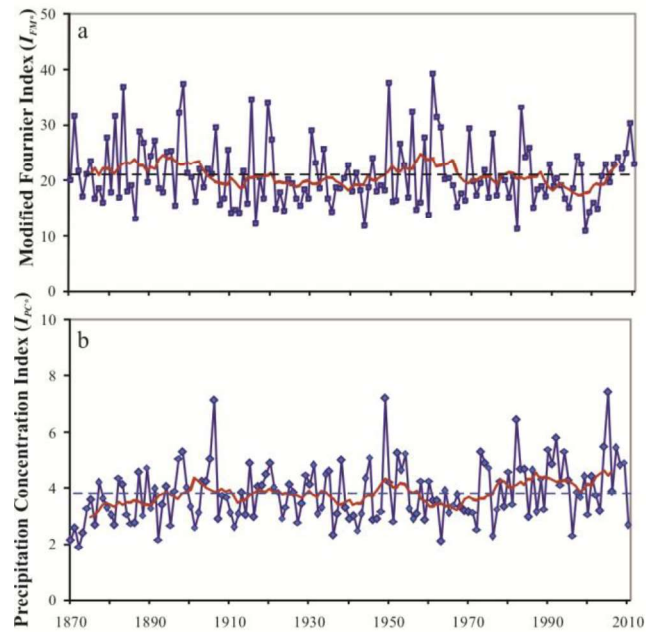
258 The methodology to calculate the  $I_D$  General Disparity Index and the  $I_{dn}$  Specific  
 259 Disparity Index is available in the Supporting Information section (S1).

#### 260 **4. Results and assessment: application to the Southwestern Iberian Peninsula**

##### 261 *4.1 Calculation of the indices $I_{FM^*}$ and $I_{PC^*}$*

262 Following the method shown in the Methodology section, to calculate  $R_A$ , it was  
 263 necessary to first calculate the annual values of the Daily Modified Fournier Index  
 264 ( $I_{FM^*}$ ) and the Daily Concentration Index ( $I_{PC^*}$ ). The values of these indices during the  
 265 period 1870-2010 were the annual components from which the corresponding  $R_A$  values  
 266 were subsequently estimated for the same period.

267 The values of  $I_{FM^*}$  and  $I_{PC^*}$  based on the ROA precipitation series for the period  
 268 1870-2010 showed no significant trend (Figure 2). Although the extreme values of both  
 269 indices occasionally coincided, generally, there was no simultaneity in the temporal  
 270 fluctuations. Values of  $I_{FM^*}$  were in a range from 10.9 to 39.3, and the actual range of  
 271 the index  $I_{PC^*}$  was 2.0 to 7.4.

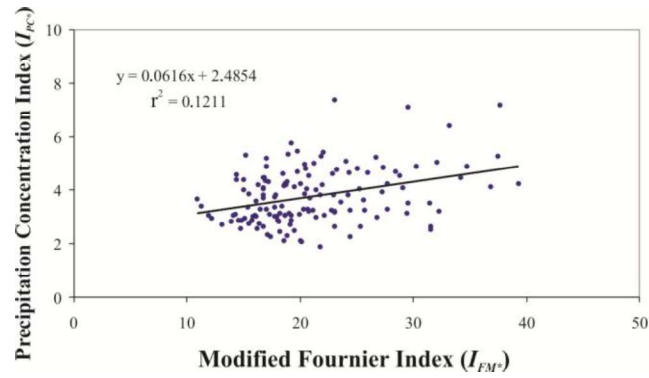


272

273 **Figure 2.a)** Temporal evolution of the  $I_{FM}^*$  and b) the  $I_{PC}^*$  showing the average value  
 274 and mobile average for periods of eleven years.

275

276 The behaviours of  $I_{FM}^*$  and  $I_{PC}^*$  have been jointly analysed year-by-year. The  $r^2$   
 277 interannual variability between  $I_{FM}^*$  and  $I_{PC}^*$  was low ( $r^2 < 0.4$ ) (T-test for Paired Values:  
 278  $T = 36.633$ ,  $T_{crit\_97.5\%} = 1.977$ ,  $p\text{-value} = 0.00 < 0.05$ ). This was confirmed in the  
 279 pairwise scatterplot that showed a wide range of points where the slightly ascending  
 280 trend explained only 12% of the total variance (Figure 3). The temporal evolutions of  
 281 both indices ( $I_{FM}^*$  and  $I_{PC}^*$ ) were therefore independent of each other, as García-Barrón  
 282 *et al.* (2015) found for the Spanish hydrographic basins. This shows that, as previously  
 283 noted, each index reflects different characteristics of the rainfall regime. With no  
 284 collinearity, it was confirmed that the respective contributions of both indices to the  
 285 calculation of the  $R_A$  are complementary.



286

287 **Figure 3.** Pairwise scatterplot of the time series  $I_{FM}^*$  and  $I_{PC}^*$  for the period 1870-2010.

288 *4.2 Characterization of the Estimated Annual Aggressiveness Risk*

289 The function  $\varphi (I_{FM}^*, I_{PC}^*)$  that establishes the balance between both indices was  
 290 obtained by multiple linear regression with respect to the local erosivity during the  
 291 interval of simultaneity (1991-2010).

292 The equation of multiple linear estimation was as follows:

293 
$$R_A = 145.24 I_{FM}^* - 341.56 I_{PC}^* \quad (9)$$

294 The determination coefficient  $r^2$  was 0.86. The substitution of values for  $I_{FM}^*$  and  
 295  $I_{PC}^*$  in equation 9 during the years of simultaneity allowed for the relation of the actual  
 296 values of the  $R$  factor to the corresponding  $R_A$  values. Figure 4 shows the relationship of  
 297 the adjustment for a level of significance  $p = 0.05$ .

298

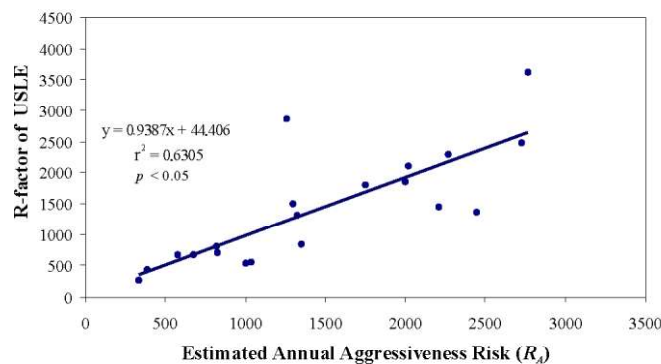
299

300

301

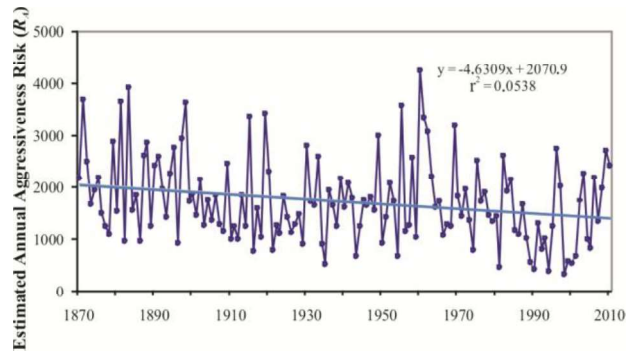
302

303



304 **Figure 4.** Pairwise scatterplot of the USLE  $R$  factor and the  $R_A$  time series for the period  
 305 1991-2010.

306 Applying equation 9 to the respective annual values of  $I_{FM}^*$  and  $I_{PC}^*$  for the  
 307 entire study period allowed extrapolation and thus generation of the interannual  
 308 estimated series of  $R_A$  from 1870 to 2010. The units for  $R_A$  are the same as those for  $R$   
 309 [(megajoules · mm) / (hectare · year hour)] and are on the same scale. Figure 5  
 310 graphically represents the evolution of the annual risk estimated for the period 1870-  
 311 2010 with the corresponding trend line.



312

313 **Figure 5.** Temporal evolution of  $R_A$  in the SW Iberian Peninsula.

314 For the entire period, the average value, the coefficient of linear trend, the  $V_n$   
 315 coefficient of variation and the  $I_D$  general disparity index of  $R_A$  were calculated. The  
 316 analysis results are shown in Table 2, which also includes the corresponding values of  
 317 the indices  $I_{FM}^*$  and  $I_{PC}^*$  for comparison purposes.

318 **Table 2.** Characterization of the  $R_A$  and its comparison to the respective statistical  
 319 components  $I_{FM}^*$  and  $I_{PC}^*$ : average, trend (linear regression), explained variance,  
 320 variability and Specific Disparity Index.

	Average	Trend	$r^2$	$V_N$	$I_D$
$I_{FM}^*$	21.0	- 0.012	< 0.01	0.28	0.40
$I_{PC}^*$	3.8	< 0.001	< 0.001	0.27	0.35
$R_A$	1742	- 4.63	< 0.1	0.47	0.64

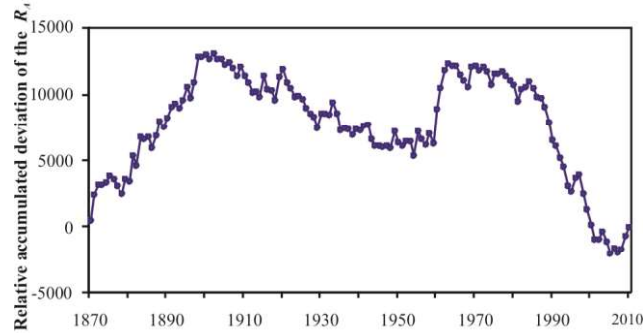


321 The average value of  $R_A$  was 1742 units. The linear trend (Figure 5) showed a  
322 slightly decreasing slope (-4.63 unit / year), statistically significant at the 95% level ( $T =$   
323  $-2.8 < -1.9$ ) but climatically not relevant because the explained variance was lower than  
324 1% ( $r^2 < 0.1$ ). Therefore, the central value was not a sufficient predictor for the temporal  
325 estimation of the  $R_A$ ; the high coefficient of variation ( $V_N = 0.47$ ) and the general  
326 disparity index ( $I_D = 0.64$ ) are proof of this state. This highlights the large temporary  
327 fluctuations of the  $R_A$  series, even between consecutive years. Additionally, the  
328 coefficient of variation and the general disparity index for  $R_A$  were higher than those for  
329  $I_{FM}^*$  and  $I_{PC}^*$ .

330 Despite the lack of a significant trend of  $R_A$ , its accumulated relative deviations  
331  $A_k$  allowed us to identify different multiannual sequences that characterized the  
332 interannual behaviour and, consequently, to identify sections of high and low risk of  
333 aggressiveness.

334 Figure 6 represents the accumulated deviations with respect to the  $\mu_N$  average of  
335 the whole series of  $R_A$ . An initial upstream line was observed until the end of the  
336 nineteenth century and involved a high frequency of years with an aggressiveness risk  
337 higher than the average of the series. This period of high frequency of the  
338 aggressiveness risk coincided with the end of the Little Ice Age in Andalusia, which led  
339 to an important clogging and reduction process in lagoons and small coastal brooks  
340 (Sousa *et al.*, 2006) in the southwestern Iberian Peninsula. Diodato *et al.* (2011) noted  
341 that erosive forces increased towards the end of the Little Ice Age (~1850) over the  
342 western and central Mediterranean in general and have increased even more during the  
343 recent warming period in meridional Mediterranean regions because of a higher  
344 frequency of intense storms. On the other hand, Figure 6 shows a downward section at

345 the first half of the 20<sup>th</sup> century, corresponding to years with aggressiveness risk below  
 346 the average and that coincided with a slightly dry period with smooth annual rainfall  
 347 fluctuations.



348

349 **Figure 6.** Evolution of the accumulated deviations with respect to the average  $R_A$ .

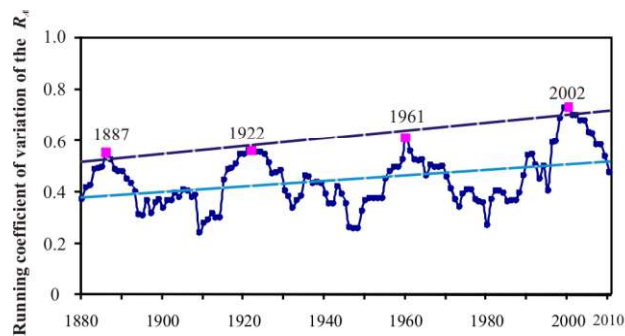
350 Finally, a steep downward phase that we associate with a period of low rainfall  
 351 aggressiveness stands out during the last thirty years of the 20<sup>th</sup> century (Figure 6). This  
 352 phase coincided with a dry period in which there was a greater dispersion of the intra-  
 353 annual rainfall, a relative lack of rainfall in spring and a shift in rainfall towards the  
 354 autumn months (García-Barrón *et al.*, 2013). Data of the erosion and silting of the  
 355 thalwegs of coastal brooks in the SW of Spain for this period show lower activity than  
 356 that for both previously mentioned periods (the end of the 19<sup>th</sup> century and the 1960s of  
 357 the 20<sup>th</sup> century), which showed high erosive activity (Figure 6). That is, phases of high  
 358 rainfall aggressiveness during the 19<sup>th</sup> and 20<sup>th</sup> centuries in the SW of Europe caused  
 359 wetland regression, especially in lagoons and coastal brooks (Sousa *et al.*, 2013, 2015).

#### 360 *4.3 Temporal irregularity of the estimated risk of aggressiveness*

361 The irregularity of the environmental effects caused by rainfall originates in the annual  
 362 and intra-annual rainfall irregularity itself. In the previous sections, we discussed the  
 363 general variability of  $R_A$  during the study period by means of  $V_N$  and  $I_D$ ; consequently, it  
 364 is necessary to analyse its interannual evolution. To do so, we calculated the mobile

365 variation coefficients for periods of eleven years ( $V_{(11)n}$ ) for the  $n$  years of the series  
 366 generated (obviously with a reduction of the first ten elements) during the observation  
 367 period.

368 The  $V_{(11)n}$  variation coefficient associated with the time sequence of the  $R_A$   
 369 annual value showed peaks of the estimated risk in the years 1887, 1922, 1961 and 2002  
 370 of approximately 0.5, separated by the corresponding periods of minimum values lower  
 371 than 0.30 (Figure 7), which indicates higher temporal stability of the interannual  $R_A$   
 372 values. This figure includes the representation of the values trend line. The last 25 years  
 373 of the series is characterized by the greatest risk variability of the 140 years studied.  
 374 Figure 7 shows a linear trend of the coefficient of variation values with a positive slope  
 375 ( $y = 0.0009x + 0.387$ ) significant for  $p = 0.05$  ( $T_C = 3.62 > 1.98$ ), with  $r^2$  equal to 0.09.  
 376 The slope increases to 0.015 in the line that links the relative maximum values (1887,  
 377 1922, 1961 and 2002).



378  
 379 **Figure 7.** Mobile variation of the  $R_A$  coefficient for periods of eleven years with the  
 380 trend line of the entire period analysed and that of the maximum relative values.

381 Therefore, the temporal analysis of  $R_A$  by means of the  $V_{(11)n}$  variation coefficient  
 382 shows an almost cyclical pattern with a pulsation of approximately 40 years (Figure 7).  
 383 This cyclical component is unique, and we have no information indicating that it had  
 384 been previously detected in the variability analysis of other climate variables in the  
 385 Mediterranean environment. Equivalent results were obtained by analysing the Specific

386 Disparity Index ( $I_{dj}$ ) are available in the Supporting Information section (S2). It is also  
387 noteworthy that the  $V_{(11)n}$  variation coefficient of the  $R_A$  presents a progressive increase  
388 of its relative extremes.

## 389 **5. Discussion**

390 The proposed methodology for calculating  $R_A$  was applied to the SW Iberian Peninsula.  
391 Temporal analysis of the generated  $R_A$  series of San Fernando (ROA, 1870-2010)  
392 showed some sequences of consecutive years that, as a whole, show a frequency of  
393 annual values higher or lower than the mean value. There was a predominance of low  
394 aggressiveness during the first half of the 20th century, especially during the last thirty  
395 years; however, there were peaks of high aggressiveness in the late 19th and mid-20th  
396 centuries coinciding with periods of high soil erosion that resulted in siltation of lagoons  
397 (Sousa *et al.*, 2013) and brooks (Sousa *et al.*, 2015) in the southwestern Iberian  
398 Peninsula (Biosphere Reserve of Doñana).

399 Although this study was developed in the Iberian Peninsula, the new parameter  
400 is based on  $I_{FM}$  and  $I_{PC}$  (indices used in different edaphic and meteorological  
401 conditions), and we consider that its application is valid for analysing the potential  
402 impacts of rainfall in different climatic and geographic areas. Thus, it is necessary to  
403 develop a weighting local equation of both indices,  $\varphi (I_{FM}^*, I_{PC}^*)$ , determined by rainfall  
404 in each region.

405 Several studies (Renard & Freid, 1994; Diodato y Bellocchi, 2007; Lee & Heo,  
406 2011; Taguas *et al.*, 2013; Yue *et al.*, 2014) have shown a high correlation between the  
407  $R$  factor and rainfall parameters such as the  $I_{FM}$ . For their part, Michiels *et al.* (1992)  
408 used the  $I_{PC}$  to analyse rainfall variability and considered that this index is appropriate  
409 for evaluating the erosivity, and Gabriels *et al.* (2003) used monthly precipitation data

410 to analyse the interannual variability of erosivity. Apaydin *et al.* (2006), Elagib (2011),  
411 Elbasit *et al.* (2013) and Meshesha *et al.* (2015) used procedures based on these indices  
412 to analyse erosivity in arid regions. Based on the  $I_{FM}$ , Sauerborn *et al.* (1999) and  
413 Nearing (2001) suggested the possibility of changes in the rainfall erosivity in Europe  
414 and the USA, respectively, during the 21<sup>st</sup> century. De Luis *et al.* (2010) separately  
415 applied  $I_{FM}$  and  $I_{PC}$  to study a possible increase in erosivity in the Spanish  
416 Mediterranean area. Additionally, both indices have been used to detect changes in the  
417 temporal trend of erosivity in southern Portugal (Nunes *et al.*, 2016) and, in an  
418 integrated way, analyse the spatial and temporal variability of aggressiveness in the  
419 watersheds of the Iberian Peninsula (García-Barrón *et al.*, 2015).

420 The advantage of the proposed methodology is that it provides an accurate  
421 annual synthesis parameter of direct interpretation, potentially applicable to different  
422 geographical areas.  $R_A$  overcomes the limitations of the intensity models because of the  
423 lack of sub-hourly records ( $R$  factor) and the imprecision of the traditional volume  
424 models ( $I_{FM}$  and  $I_{PC}$ ) associated with the effects of heavy rainfall episodes. Therefore,  
425 the new  $R_A$  parameter is an appropriate mechanism for estimating the potential  
426 environmental impact of rainfall aggressiveness and for performing spatial and temporal  
427 comparative analysis.

428 To determine the equation  $\varphi (I_{FM}, I_{PC})$  with sufficient accuracy, we needed  
429 minimum simultaneous daily and sub-hourly rainfall records in addition to local erosion  
430 data. An open research line for the future is to extend the application of this  
431 methodology to other study areas with different climatic conditions, particularly in the  
432 Mediterranean, semiarid environments and environments at risk of desertification, and  
433 to compare the results to the results obtained by other methods and at other time scales.

434 Although the proposed methodology has theoretical foundations, it would be convenient  
435 to establish a direct empirical verification of  $R_A$  to allow for the quantification of rainfall  
436 environmental impacts (runoff, siltation of wetlands, etc.). Another aspect to consider is  
437 that although  $R_A$  estimates the rainfall potential energy, the erosive process is much  
438 more complex, and it is not always that rainfall amount and/or distribution the main  
439 factor affecting the erosive process. García-Ruiz *et al.* (2015) conducted a worldwide  
440 meta-analysis of soil erosion rates, based on data from more than 4000 sites, whose  
441 results show that there is extraordinarily high variability in erosion rates, with almost  
442 any rate apparently possible irrespective of land slope, climate, scale, land use/land  
443 cover and other environmental characteristics. Despite this variability, some general  
444 trends were found, including an increase in erosion rates with increasing land slope and  
445 annual precipitation, the association of agricultural practices with the highest erosion  
446 rates, and a correlation between shrub coverage and the lowest erosion rates. Even so,  
447 the worldwide meta-analysis of García-Ruiz *et al.* (2005) suggests that only order of  
448 magnitude approximations of erosion rates are possible. This supposes a high degree of  
449 uncertainty and causes these authors to postulate the need to develop protocols that  
450 allow the comparison of the results of different sites.

451 Human activity can also significantly affect the development and evolution of  
452 denudation hot spots, especially through changes in land use (Vergari *et al.*, 2013). As  
453 these authors point out, this factor has a great importance associated with the croplands  
454 abandonment, and in general, in badlands of the Mediterranean area. The relationships  
455 among the various factors that influence the erosion intensity are very complex, and  
456 therefore new studies are needed to continue to deepen these aspects, with the support  
457 of real erosion measures taken directly from the field work.

## 458 **6. Conclusions**

459 A new synthesis parameter  $R_A$  was calculated by means of the combined use of the  
460 Fournier ( $I_{FM}^*$ ) and Oliver concentration ( $I_{PC}^*$ ) indices and reformulated with daily data.  
461 Weighting between both indices was obtained by multiple regression with the local  
462 erosivity. The historical extrapolation allowed the interannual series of the  $R_A$  to be  
463 obtained. A comparative analysis of the temporal evolution of  $I_{FM}^*$  and  $I_{PC}^*$  showed that  
464 they were independent of each other and that their contributions to the calculation of  $R_A$   
465 were complementary. Obtaining the annual values of  $R_A$  in the same units and scale as  
466 the USLE  $R$  function allowed for the generalization of the results, thus increasing their  
467 applicability and establishing a link among historical rainfall records and current values  
468 of the potential rainfall aggressiveness.

469 In our opinion, the proposed methodology has the ability to provide consistent  
470 conclusions about historical erosive processes in each region linked to the potential  
471 rainfall aggressiveness. Therefore, it has a special relevance to the design of  
472 environmental measures and land management policies that prevent the direct and  
473 indirect impacts of rainfall.

## 474 **7. Acknowledgements**

475 We would like to thank the Navy's Royal Observatory of San Fernando (ROA) for  
476 providing the rainfall records and the Environmental Information Network of the  
477 Ministry of Environment of the Junta de Andalucía for providing the data set to  
478 calculate the erosivity. We thank María Ángeles Garrido and Alicia Cebolla for their  
479 help in data processing.

## 480 **8. References**

- 481 Aguilar M. 2007. Recent changes and tendencies in precipitation in Andalusia. In:  
482 Climate Change in Andalusia: trends and environmental consequences, Sousa A,  
483 García-Barrón L, Jurado V. (eds). Consejería de Medio Ambiente: Sevilla; 99-  
484 116. <https://idus.us.es/xmlui/handle/11441/30483>
- 485 Alexandersson H. 1986. A homogeneity test applied to precipitation data. *Journal of*  
486 *Climatology* **6**: 661- 675. DOI:10.1002/joc.3370060607.
- 487 Almarza C, López A, Flores C. 1996. Homogeneidad y variabilidad de los registros  
488 históricos de precipitación en España. Instituto Nacional de Meteorología,  
489 Madrid.
- 490 Angulo-Martínez M, López-Vicente M, Vicente-Serrano SM, Beguería S. 2009.  
491 Mapping rainfall erosivity at a regional scale, a comparison of interpolation  
492 methods in the Ebro Basin (NE Spain). *Hydrology and Earth System Sciences*  
493 **13**: 1907-1920. DOI:10.5194/hess-13-1907-2009.
- 494 Apaydin H, Erpul G, Bayramin I, Gabriels D. 2006. Evaluation of indices for  
495 characterizing the distribution and concentration of precipitation: a case for the  
496 region of Southeastern Anatolia Project, Turkey. *Journal of Hydrology* **328**:  
497 726-732. DOI:10.1016/j.jhydrol.2006.01.019.
- 498 Arnoldus HMJ. 1980. An approximation of the rainfall factor in the universal soil loss  
499 equation. In: Assessment of Erosion, De Boodt M, Gabriels D (eds). John Wiley:  
500 Chichester; 127-132.
- 501 Da Silva AM. 2004. Rainfall erosivity map for Brazil. *Catena* **57**: 251-259.  
502 DOI:10.1016/j.catena.2003.11.006.



- 503 De Luis M, Gonzalez-Hidalgo JC, Longares LA. 2010. Is rainfall erosivity increasing in  
 504 the Mediterranean Iberian Peninsula? *Land Degradation & Development* **21**:  
 505 139-144. DOI:10.1002/ldr.918.
- 506 Diodato N, Bellocchi G, Romano N, Chirico GB. 2011. How the aggressiveness of  
 507 rainfalls in the Mediterranean lands is enhanced by climate change. *Climatic*  
 508 *Change* **108**: 591-599. DOI:10.1007/s10584-011-0216-4.
- 509 Diodato N, Bellocchi G. 2007. Estimating monthly (R)USLE climate input in a  
 510 Mediterranean region using limited data. *Journal of Hydrology* **345**: 224-236.  
 511 DOI:10.1016/j.jhydrol.2007.08.008.
- 512 Diodato N, Ceccarelli M, Bellocchi G. 2008. Decadal and century-long changes in the  
 513 reconstruction of erosive rainfall anomalies in a Mediterranean fluvial basin.  
 514 *Earth Surface Processes and Landforms* **33**: 2078-2093. DOI: 10.1002/esp.1656.
- 515 Elagib NA. 2011. Changing rainfall, seasonality and erosivity in the hyper-arid zone of  
 516 Sudan. *Land Degradation & Development* **22**: 505–512. DOI:10.1002/ldr.1023.
- 517 Elbasit AMA, Ojha CSP, Jinbai H, Yasuda H, Kimura R, Ahmed Z. 2013. Relationship  
 518 between rainfall erosivity indicators under arid environments: Case of  
 519 Liudaogou basin in Chinese Loess Plateau. *Journal of Food, Agriculture &*  
 520 *Environment* **11**: 1073-1077. [http://world-food.net/download/journals/2013-](http://world-food.net/download/journals/2013-issue_2/2013-issue_2-environment/e55.pdf)  
 521 [issue\\_2/2013-issue\\_2-environment/e55.pdf](http://world-food.net/download/journals/2013-issue_2/2013-issue_2-environment/e55.pdf).
- 522 Fournier F. 1960. Climat et érosion. Presse Universitaire de France, Paris.
- 523 Gabriels D, Vermeulen A, Verbist K, Van Meirvenne M. 2003. Assessment of rain  
 524 erosivity and precipitation concentration in Europe. In: Proceedings of the  
 525 International Symposium, 25 Years of Assessment of Erosion, Gabriels D,  
 526 Cornelis W (eds). Ghent; 87–92.

- 527 García-Barrón L, Aguilar M, Sousa A. 2011. Evolution of annual rainfall irregularity in  
 528 the southwest of the Iberian Peninsula. *Theoretical and Applied Climatology*  
 529 **103**: 13-26. DOI:10.1007/s00704-010-0280-0.
- 530 García-Barrón L, Camarillo JM, Morales J, Sousa A. 2015. Temporal analysis (1940–  
 531 2010) of rainfall aggressiveness in the Iberian Peninsula basins. *Journal of*  
 532 *Hydrology* **525**: 747-759. DOI:10.1016/j.jhydrol.2015.04.036.
- 533 García-Barrón L, Morales J, Sousa A. 2013. Characterisation of the intra-annual rainfall  
 534 and its evolution (1837-2010) in the southwest of the Iberian Peninsula.  
 535 *Theoretical and Applied Climatology* **114**: 445-457. DOI:10.1007/s00704-013-  
 536 0855-7.
- 537 García-Ruiz JM, Beguería S, Nadal-Romero E, González-Hidalgo JC, Lana-Renault N,  
 538 Sanjuán Y. 2015. A meta-analysis of soil erosion rates across the world.  
 539 *Geomorphology* **239**: 160-173. DOI:10.1016/j.geomorph.2015.03.008.
- 540 García-Ruiz JM, Nadal-Romero E, Lana-Renault N, Beguería S. 2013. Erosion in  
 541 Mediterranean landscapes: changes and future challenges. *Geomorphology* **198**:  
 542 20-36. DOI:10.1016/j.geomorph.2013.05.023.
- 543 Gregori E, Costanza M, Zorn G. 2006. Assessment and classification of climatic  
 544 aggressiveness with regard to slope instability phenomena connected to  
 545 hydrological and morphological processes. *Journal of Hydrology* **329**: 489–499.  
 546 DOI:10.1016/j.jhydrol.2006.03.001.
- 547 Hernando D, Romana MG. 2016. Estimate of the (R)USLE rainfall erosivity factor from  
 548 monthly precipitation data in mainland Spain. *Journal of Iberian Geology* **42**:  
 549 113-124. DOI:10.5209/rev\_JIGE.2016.v42.n1.49120.

- 550 ICONA 1988. Agresividad de la lluvia en España. Valores del factor R de la ecuación  
 551 universal de pérdidas de suelo. Servicio de Publicaciones del Ministerio de  
 552 Agricultura, Pesca y Alimentación, Madrid.
- 553 Kinnell P. 2010. Event soil loss, runoff and the Universal Soil Loss Equation family of  
 554 models: A review. *Journal of Hydrology* **385**: 384–397.  
 555 DOI:10.1016/j.jhydrol.2010.01.024.
- 556 Lee JH, Heo JH. 2011. Evaluation of estimation methods for rainfall erosivity based on  
 557 annual precipitation in Korea. *Journal of Hydrology* **409**: 30-48.  
 558 DOI:10.1016/j.jhydrol.2011.07.031.
- 559 Loureiro NS, Couthino MA. 2001. A new procedure to estimate the RUSLE EI30 index,  
 560 based on monthly rainfall data applied to the Algarve region, Portugal. *Journal*  
 561 *of Hydrology* **250**: 12-18. DOI:10.1016/S0022-1694(01)00387-0.
- 562 Martín-Vide J, López-Bustins JA. 2006. The western Mediterranean oscillation and  
 563 rainfall in the Iberian Peninsula. *International Journal of Climatology* **26**: 1455-  
 564 1475. DOI:10.1002/joc.1388.
- 565 Martín-Fernández L, Martínez-Núñez M. 2011. An empirical approach to estimate soil  
 566 erosion risk in Spain. *Science of the Total Environment* **409**: 3114-3123.  
 567 <http://doi.org/10.1016/j.scitotenv.2011.05.010>
- 568 Meshesha DT, Tsunekawa A, Tsubo M, Haregeweyn N, Adgo E. 2015. Evaluating  
 569 spatial and temporal variations of rainfall erosivity, case of Central Rift Valley  
 570 of Ethiopia. *Theoretical and Applied Climatology* **119**: 515-522.  
 571 DOI:10.1007/s00704-014-1130-2.

- 572 Michiels P, Gabriels D, Hartmann R. 1992. Using the seasonal and temporal  
 573 precipitation concentration index for characterizing monthly rainfall distribution  
 574 in Spain. *Catena* **19**: 43-58. DOI:10.1016/0341-8162(92)90016-5.
- 575 Nearing MA. 2001. Potential changes in rainfall erosivity in the US with climate change  
 576 during the 21st century. *Journal of Soil and Water Conservation* **56**: 229-232.
- 577 Nunes AN, Lourenço L, Vieira A, Bento-Gonçalves A. 2016. Precipitation and erosivity  
 578 in southern Portugal: seasonal variability and trends (1950–2008). *Land*  
 579 *Degradation & Development* **27**: 211-222. DOI:10.1002/ldr.2265.
- 580 Oliver JE. 1980. Monthly precipitation distribution, a comparative index. *The*  
 581 *Professional Geographer* **32**: 300–309. DOI:10.1111/j.0033-0124.1980.00300.x.
- 582 Panagos P, Ballabio C, Borrelli P, Meusburger K, Klik A, Rousseva S, Tadic MP,  
 583 Michaelides S, Hrabalíková M, Olsen P, Aalto J, Lakatos M, Rymaszewicz A,  
 584 Dumitrescu A, Beguería S, Alewell C. 2015. Rainfall erosivity in Europe.  
 585 *Science of the Total Environment* **511**: 801-814.  
 586 DOI:10.1016/j.scitotenv.2015.01.008.
- 587 Renard KG, Foster GR, Weesies GA, McCool DK, Yoder DC. 1997. Predicting soil  
 588 erosion by water: A guide to conservation planning with the Revised Universal  
 589 Soil Loss Equation (RUSLE). Agriculture Handbook 703, USDA.
- 590 Renard KG, Freid JR. 1994. Using monthly precipitation data to estimate the *R* factor in  
 591 the revised USLE. *Journal of Hydrology* **157**: 287-306. DOI:10.1016/0022-  
 592 1694(94)90110-4.
- 593 Rodrigo FS. 2002. Changes in climate variability and seasonal rainfall extremes: a case  
 594 study from San Fernando (Spain), 1821–2000. *Theoretical and Applied*  
 595 *Climatology* **72**: 193-207. DOI:10.1007/s007040200020.

- 596 Rodríguez Surián M, Sánchez Pérez JD. 1995. Distribución espacio-temporal de las  
 597 pérdidas de suelo en Andalucía utilizando tecnología S.I.G. e imágenes de  
 598 satélite.  
 599 [http://www.juntadeandalucia.es/medioambiente/web/Red\\_informacion\\_ambien](http://www.juntadeandalucia.es/medioambiente/web/Red_informacion_ambienta)  
 600 [ta/l/productos/Publicaciones/articulos/articulos\\_pdf/Distespa.pdf](http://www.juntadeandalucia.es/medioambiente/web/Red_informacion_ambienta/l/productos/Publicaciones/articulos/articulos_pdf/Distespa.pdf).
- 601 Sánchez-Canales M, López-Benito A, Acuña V, Ziv G, Hamel P, Chaplin-Kramer R,  
 602 Elorza FJ. 2015. Sensitivity analysis of a sediment dynamics model applied in a  
 603 Mediterranean river basin: Global change and management implications. *Science*  
 604 *of the Total Environment* **502**: 602-610.  
 605 <http://doi.org/10.1016/j.scitotenv.2014.09.074>.
- 606 Sanchez-Moreno JF, Mannaerts CM, Jettena V. 2014. Rainfall erosivity mapping for  
 607 Santiago Island, Cape Verde. *Geoderma* **217**: 74-82.  
 608 DOI:10.1016/j.geoderma.2013.10.026.
- 609 Sauerborn P, Klein A, Botschek J, Skowronek A. 1999. Future rainfall erosivity derived  
 610 from large-scale climate models—methods and scenarios for a humid region.  
 611 *Geoderma* **93**: 269-276. DOI:10.1016/S0016-7061(99)00068-3.
- 612 Solé A. 2006. Spain. In: Soil Erosion in Europe, Boardman J, Poesen J (eds). John  
 613 Wiley & Sons; 311–346.
- 614 Sousa A, García-Barrón L, García-Murillo P, Vetter, Morales J. 2015. The use of  
 615 changes in small coastal Atlantic brooks in southwestern Europe as indicators of  
 616 anthropogenic and climatic impacts over the last 400 years. *Journal of*  
 617 *Paleolimnology* **53**: 73-88. DOI:10.1007/s10933-014-9809-z

- 618 Sousa A, García-Barrón L, Morales J, García-Murillo P. 2006. Post-Little Ice Age  
 619 warming and desiccation of the continental wetlands of the Aeolian sheet in the  
 620 Huelva region (SW Spain). *Limnetica* **25**: 57-70.
- 621 Sousa A, García-Murillo P, Morales J, García-Barrón L. 2009. Anthropogenic and  
 622 natural effects on the coastal lagoons in the southwest of Spain (Doñana  
 623 National Park). *ICES Journal of Marine Science* **66**: 1508-1514.  
 624 DOI:10.1093/icesjms/fsp106.
- 625 Sousa A, Morales J, García-Barrón L, García-Murillo P. 2013. Changes in the *Erica*  
 626 *ciliaris* Loeffl. ex L. peat bogs of southwestern Europe from the 17<sup>th</sup> to the 20<sup>th</sup>  
 627 centuries AD. *Holocene* **23**: 255-269. DOI:10.1177/0959683612455545.
- 628 Stepanek P. 2007. AnClim—software for time series analysis (for  
 629 Windows). Department of Geography, Faculty of Natural Sciences, Masaryk  
 630 University, Brno.
- 631 Taguas EV, Carpintero E, Ayuso JL. 2013. Assessing land degradation risk through the  
 632 long-term analysis of erosivity: a case study in southern Spain. *Land*  
 633 *Degradation & Development* **24**: 179-187. DOI:10.1002/ldr.1119.
- 634 Terranova O, Antronico L, Coscarelli R, Iaquina P. 2009. Soil erosion risk scenarios in  
 635 the Mediterranean environment using RUSLE and GIS: an application model for  
 636 Calabria (southern Italy). *Geomorphology* **112**: 228-245.  
 637 DOI:10.1016/j.geomorph.2009.06.009.
- 638 Vergari F, Della Seta M, Del Monte M, Fredi P, Palmieri EL. 2013. Long-and short-  
 639 term evolution of several Mediterranean denudation hot spots: The role of  
 640 rainfall variations and human impact. *Geomorphology* **183**: 14-27. DOI:  
 641 10.1016/j.geomorph.2012.08.002.

- 642 Wischmeier WH, Smith DD. 1978. Predicting rainfall erosion loss: a guide to  
643 conservation planning. Agriculture Handbook 537, Washington.
- 644 Yue BJ, Shi ZH, Fang NF. 2014. Evaluation of rainfall erosivity and its temporal  
645 variation in the Yanhe River catchment of the Chinese Loess Plateau. *Natural*  
646 *Hazards* 74: 585-602. DOI:10.1007/s11069-014-1199-z.
- 647

648 **Table 1.** Proportionality coefficient and annual and interannual correlation between the  
 649 San Fernando Observatory (ROA) and the selected regional stations

<b>Observatories</b>	<b>Country</b>	<b>Institution</b>	<b>Latitude and Longitude</b>	<b>Annual average rate</b>	<b>R-Pearson Interannual</b>	<b>R-Pearson Intra-annual</b>
San Fernando (ROA)	Spain	ROA	36° 27' 56" N 6° 12' 20" W	-	-	-
Cadiz	Spain	AEMET	36° 32' 01" N 6° 17' 58" W	1.04	0.96	1.00
Huelva	Spain	AEMET	37° 16' 30" N 6° 54' 35" W	1.03	0.94	0.98
Faro	Portugal	IPMA	37° 01' 00" N 7° 55' 59" W	1.04	0.76	0.97
Seville	Spain	AEMET	37° 25' 05" N 5° 42' 30" W	1.02	0.85	0.98
Cordova	Spain	AEMET	37° 50' 40" N 4° 51' 02" W	0.96	0.86	0.98
Badajoz	Spain	AEMET	38° 43' 02" N 6° 49' 45" W	1.02	0.72	0.94
Beja	Portugal	IPMA	38° 00' 56" N 7° 51' 55" W	0.92	0.70	0.94

650

651



652 **Table 2.** Characterization of the  $R_A$  and its comparison to the respective statistical  
 653 components  $I_{FM^*}$  and  $I_{PC^*}$ : average, trend (linear regression), explained variance,  
 654 variability and *Specific Disparity Index*

	<b>Average</b>	<b>Trend</b>	$r^2$	$V_N$	$I_D$
$I_{FM^*}$	21.0	- 0.012	< 0.01	0.28	0.40
$I_{PC^*}$	3.8	< 0.001	< 0.001	0.27	0.35
$R_A$	1742	- 4.63	< 0.1	0.47	0.64

655

656

657

**FIGURE LEGEND**

658 Figure 1. Map showing the locations of the meteorological stations used in the study  
659 area.

660 Figure 2.a) Temporal evolution of the  $I_{FM}^*$  and b) the  $I_{PC}^*$  showing the average value  
661 and mobile average for periods of eleven years.

662 Figure 3. Pairwise scatterplot of the time series  $I_{FM}^*$  and  $I_{PC}^*$  for the period 1870-2010.

663 Figure 4. Pairwise scatterplot of the USLE  $R$  factor and the  $R_A$  time series for the period  
664 1991-2010.

665 Figure 5. Temporal evolution of  $R_A$  in the SW Iberian Peninsula.

666 Figure 6. Evolution of the accumulated deviations with respect to the average  $R_A$ .

667 Figure 7. Mobile variation of the  $R_A$  coefficient for periods of eleven years with the  
668 trend line of the entire period analysed and that of the maximum relative values.

669